ACS OMEGA

Open Access

http://pubs.acs.org/journal/acsodf

Article

Soyasaponin Bb/Gelatin-Methacryloyl Hydrogel for Cartilage Inflammation Inhibition

Yuhan Jiang, Tenghai Li, Bingzhang Liu, Yufeng Tian, Yixin Wang, Tian Li,* and Duo Zhang*

Cite This: *ACS Omega* 2024, 9, 49597−49608

Read Online

ACCESS | Metrics & More | Article Recommendations | Supporting Information

ABSTRACT: The main causes of failure for cartilage tissue engineering implants are tissue integration, inflammation, and infection. The development of biomaterials with antiforeign body response (FBR) is of particular importance. Herein, we developed a hydrogel loaded with anti-inflammatory drugs to reduce the inflammatory response that follows implantation. The human chondrocytes were used for in vitro study, and cell-laden hydrogel samples were implanted with the backs of rabbits for in vivo study. Soyasaponin Bb (SsBb) as a traditional Chinese medicine could significantly ($P < 0.05$) downregulate the expression levels of inflammation-related markers including iNOS, COX-2, and IL-6 in chondrocytes induced by IL-1β through the NF-κB signaling pathway. The in vitro experiments demonstrated that a gelatin-methacryloyl (GelMA) hydrogel loaded with SsBb (SsBb/GelMA) could similarly reduce the gene and protein expression levels of inflammation-related markers (iNOS, COX-2, and IL-6). The in vivo anti-inflammatory effects of the SsBb/GelMA hydrogels were assessed by immunohistochemical staining. The results demonstrated that SsBb/GelMA hydrogels inhibited the inflammatory response and downregulated the expression of the inflammatory cytokine IL-6. Therefore, SsBb/GelMA hydrogels are promising candidates for promoting anti-inflammation and cartilage tissue regeneration of implant surfaces.

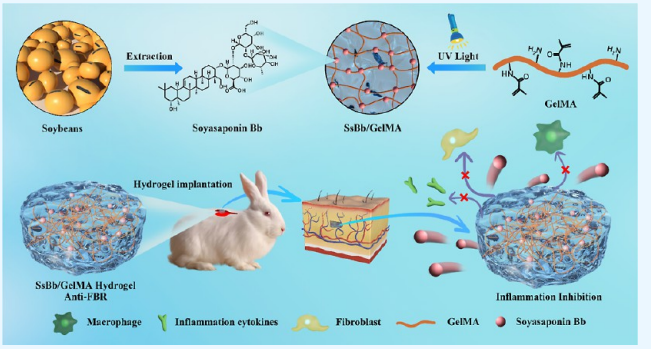

1. INTRODUCTION

The majority of cartilage abnormalities are caused by aging, disease, or trauma-related cartilage lesions. The distinct structural features of cartilage, such as its lack of blood arteries, nerves, and lymphatic vessels, make full recovery from damage exceedingly challenging.[1] Current clinical treatments including microfracture (marrow stimulation), autologous chondrocyte implantation,[2,3] and osteochondral autografts are not very effective.[4−6] In recent years, the rapid development of tissue engineering has greatly promoted the process of cartilage regeneration.[7] However, the foreign body reaction (FBR) significantly decreases the stability of cartilage construction during the tissue engineering process. A series of biological reactions known as FBR are caused by implantable biomaterials that the host immune system recognizes as a foreign object at the implant−host interface. These reactions include strong inflammatory responses, the formation of foreign-body giant cells, fibrosis, and ultimately collagen encapsulation around the implants, which isolates the implants from the host tissue.[8−11]

Following biomaterial implantation, the healing process is comparable to wound healing in that the provisional matrix acts initially. The provisional matrix is formed by the deposition of blood proteins on the surface of biomaterials, in which biologically active factors such as mitogens, chemoattractants, cytokines, growth factors, etc., are present, which provide a rich environment for inflammatory response.[11,12] Therefore, the development of anti-FBR biomaterials is imperative. Anti-FBR biomaterials are required to guarantee biocompatibility while facilitating tissue regeneration and repair and regulating the inflammatory milieu, which includes inflammatory cytokines. Besides, the anti-FBR biomaterials need to be easily synthesized, stably stored, and transported with low cost.[13−15] Hydrogels are a class of highly hydrophilic, three-dimensional, lattice-like structured gels with excellent biocompatibility and biodegradability. Hydrogels are ideal vehicles for drug delivery and widely used in biomedical applications.[16,17] Gelatin-methacryloyl (GelMA) is a photosensitive biomaterial synthesized from gelatin and methacrylic anhydride (MA) with excellent biocompatibility and has been widely used in various biological applications, including scaffolds, tissue repair, and drug delivery.[18,19]

Soyasaponins (SSs) are the major phytochemicals found in soybeans and soy products, categorized into several subtypes,

Received: August 16, 2024
Revised: October 8, 2024
Accepted: November 27, 2024
Published: December 4, 2024

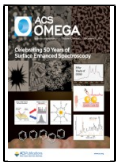

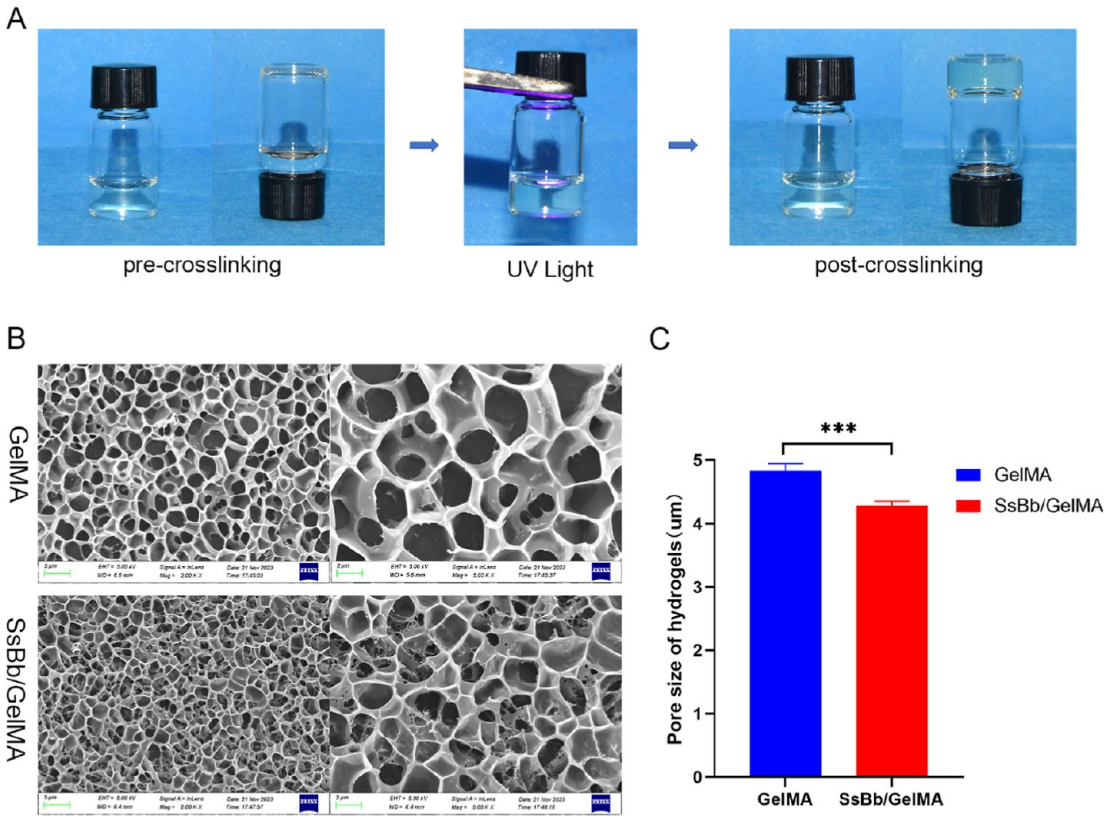

Figure 1. Surface morphology and structure of hydrogels. (A) The process of cross-linking of GelMA hydrogels. (B) The SEM images of GelMA and SsBb/GelMA hydrogels. (C) The average pore size of GelMA and SsBb/GelMA hydrogels. ***$p < 0.001$.

including A, B, E, and DMMP (2,3-dihydro-2,5-dihydroxy-6-methyl-4*H*-pyran-4-one).[20] It has been shown that SSs have biological properties that include anti-inflammatory, antioxidant, hepatoprotective, hypolipidemic, antiviral, and anticancer effects.[21] Soyasaponin Bb (SsBb), as one of the most abundant subtypes in soybeans, has been shown to have anti-inflammatory effects.[22−24] SsBb not only downregulates the expression levels of inflammation-related markers including IL-6, COX-2, TNF-a, and IL18 but also inhibits matrix degradation. However, the anti-inflammatory role of SsBb in tissue-engineered cartilage construction has not been investigated. The systematic inflammation can be induced by triggering IL-1β secretion through the inflammasome pathway.[25] Thus, IL-1β was used in this study to induce inflammation. And the anti-inflammatory effect was then explored by the addition of SsBb.

In this study, we demonstrated the anti-inflammatory effects of SsBb in chondrocytes, which downregulates the expression of inflammation-related markers through the NF-κB pathway. SsBb can be used to regulate the tissue microenvironment, reduce the FBR by implanted hydrogels, and promote tissue repair and regeneration. The anti-inflammatory biomaterial SsBb/GelMA hydrogel was constructed, and its physicochemical properties were investigated. Furthermore, in vitro and in vivo experiments were used to evaluate the anti-inflammatory effects of SsBb/GelMA hydrogels.

2. RESULTS

2.1. Characterization of GelMA and SsBb/GelMA Hydrogel. The surface morphology and structure of GelMA and the SsBb/GelMA hydrogels were studied. The fabrication process of the hydrogel is shown in Figure 1A. In order to detect the internal structure of GelMA and SsBb/GelMA hydrogel scaffolds, SEM was applied and confirmed the porous structure of the two scaffolds (Figure 1B). The average pore size of the GelMA hydrogel was 4.83 ± 0.11 μm, and that of the SsBb/GelMA hydrogel was 4.29 ± 0.06 μm (Figure 1C). The average pore size of GelMA hydrogels was larger than that of SsBb/GelMA hydrogels with a statistically significant difference.

2.2. Swelling, Degradation Ratio, and Mechanical Strength of GelMA and SsBb/GelMA Hydrogel. To test the swelling rate, both groups of hydrogels were soaked in PBS for 12, 24, and 48 h (Figure 2A). Both groups of hydrogels reached a maximum swelling ratio around 12 h, with a maximum swelling ratio of 120% for GelMA and 118% for SsBb/GelMA, indicating no significant difference. In the degradation test within 28 days, both groups of hydrogels underwent slow and stable degradation. At the 28th day, the degradation rate of hydrogels in GelMA hydrogels reached about 40%, while the degradation rate of SsBb/GelMA hydrogels was slightly lower at 36% (Figure 2B).

To study the mechanical strength of GelMA and SsBb/GelMA hydrogels, compression tests were carried out using a universal mechanical testing machine (Figure 2C,D). The compression ratios were 16.73 ± 0.55 KPa for the GelMA hydrogels and 18.97 ± 0.31 KPa for the SsBb/GelMA hydrogels. The compression stress of the SsBb/GelMA hydrogels was stronger than that of the GelMA hydrogels with a statistical difference.

2.3. Drug Release and Fourier Infrared Spectroscopy of the SsBb/GelMA Hydrogel. High-performance liquid

https://doi.org/10.1021/acsomega.4c07489
ACS Omega 2024, 9, 49597−49608

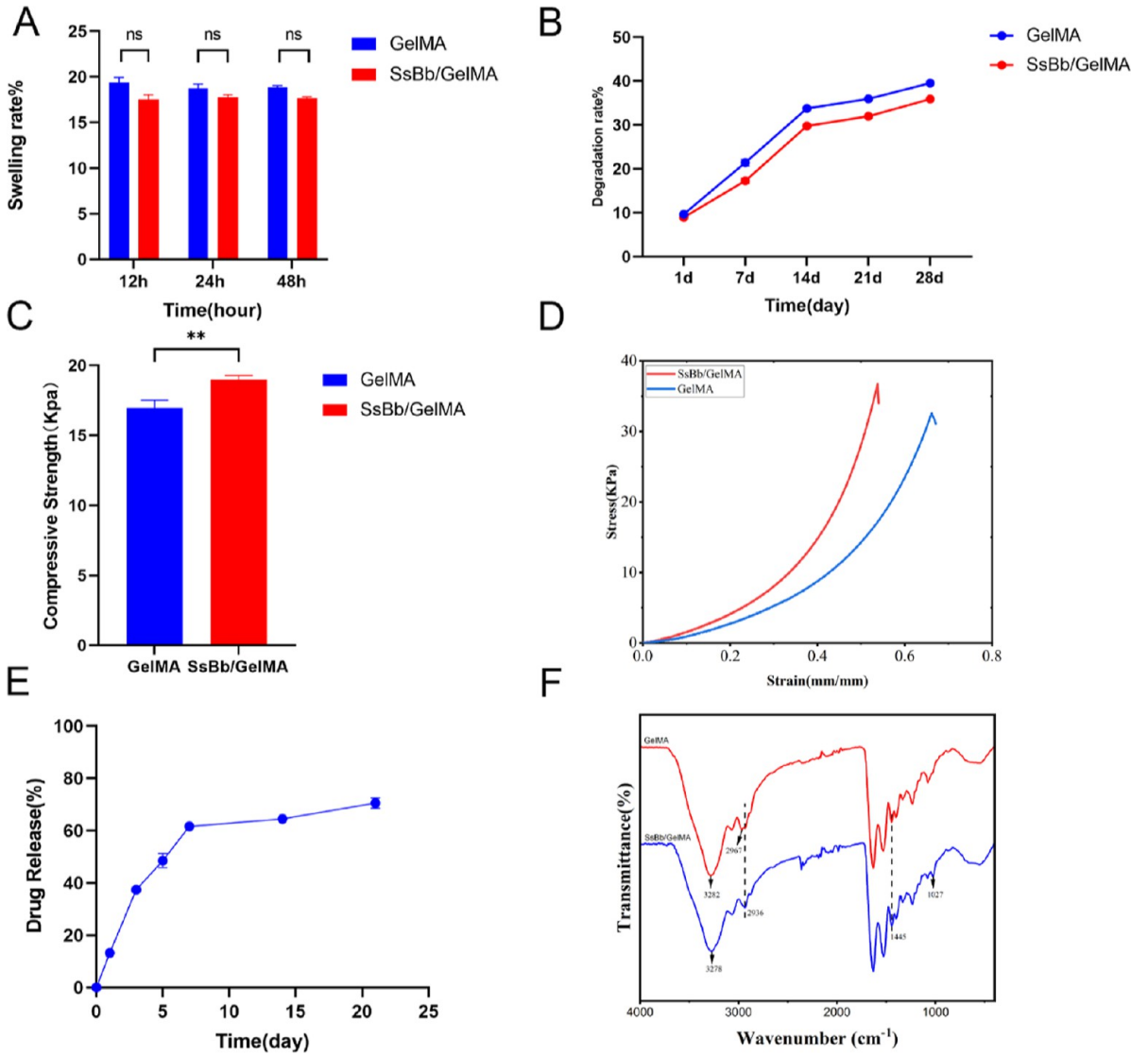

Figure 2. Characterization of GelMA and SsBb/GelMA hydrogels. (A) Swelling test of GelMA and SsBb/GelMA hydrogels. (B) Degradation test of GelMA and SsBb/GelMA hydrogels. (C,D) Compression test of GelMA and SsBb/GelMA hydrogels. (E) Drug release of the SsBb/GelMA hydrogel. (F) Fourier infrared detection of GelMA and SsBb/GelMA hydrogels. $^{**}p < 0.01$; ns, no significance.

chromatography (HPLC) was used to detect the drug release of the SsBb/GelMA hydrogel. The maximum absorption wavelength of SsBb is around 207 nm. SsBb in SsBb/GelMA was continuously released during 21 days of the assay. Notably, there was a sharp release of SsBb during 0−7 d. But after 7 d, there was a slow release of SsBb, with the percentage of drug release reaching 70% at the 21st day (Figure 2E).

As shown in Figure 2F, the curve directions of GelMA and SsBb/GelMA hydrogels are roughly similar but slightly different. It can be seen that in the SsBb/GelMA hydrogel curve, the absorption peak representing the N−H stretching vibration is shifted from 3282 to 3278 cm^{-1}, which suggests that hydrogen bonding has occurred between the substances, resulting in the lengthening of the bond lengths of the N−H and O−H bonds. Not only that, but also the intensity of the absorption peak at 2974 cm^{-1} is weakened, while the intensity of the absorption peaks representing the methylene stretching vibration and the variable angle vibration at 2935 and 1446 cm^{-1} is increased, which is due to the introduction of the methylene group in SsBb. A new absorption peak appeared at 1027 cm^{-1}, which was caused by the stretching vibration of herbal alcohol C−O. The results proved that SsBb was successfully introduced into the GelMA hydrogel.

2.4. SsBb Inhibits Inflammation of Chondrocytes. To determine the cytotoxic effect of SsBb, human passage 2 (P2) chondrocytes were exposed to SsBb at different concentrations (0, 1, 5, 10, 25, 50, and 100 μg/mL) and DMSO for 24, 48, or 72 h (Figure 3A). SsBb did not show significant cytotoxicity to chondrocytes at a concentration below 10 μg/mL after 24, 48, and 72 h. For subsequent studies, different concentrations (1, 5, and 10 μg/mL) of SsBb were used.

The effect of SsBb on IL-1β-mediated inflammation was determined by assaying several inflammation-related markers in human P2 chondrocytes. Elevated protein expression of inflammation-related markers including iNOS, COX-2, and IL-6 was confirmed by Western blot. In contrast, protein expression levels were decreased with the treatment of SsBb (Figure 3B,C). The q-PCR results were consistent with those of Western blot analysis (Figure 3D). It is worth noting that there was no statistical difference in the anti-inflammatory

https://doi.org/10.1021/acsomega.4c07489
ACS Omega 2024, 9, 49597−49608

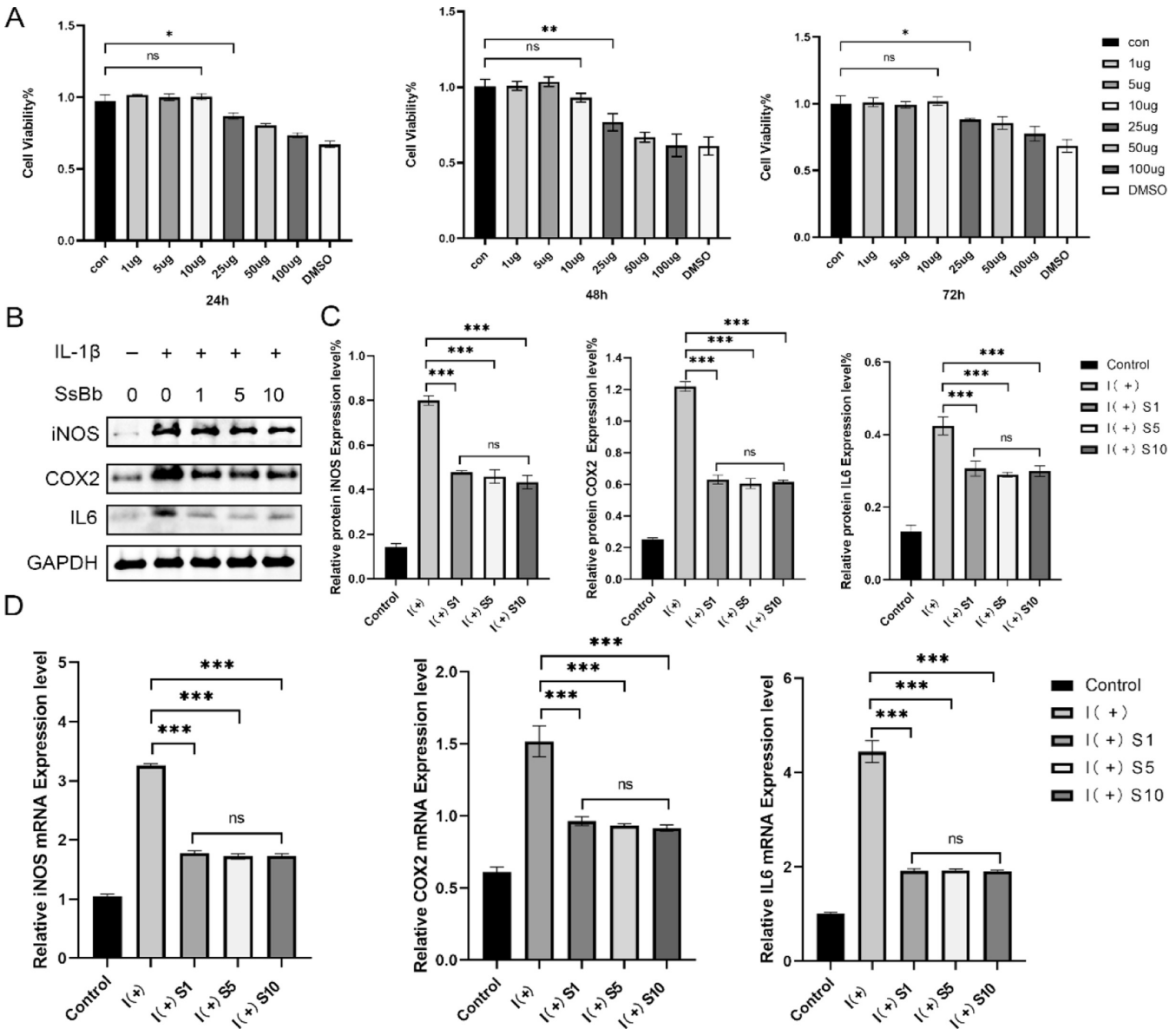

Figure 3. Soyasaponin Bb's protective effects against inflammation induced by IL-1β. (A) The human P2 chondrocytes were pretreated with increasing concentrations of SsBb (1, 5, 10, 25, 50, and 100 μg/mL) for 24, 48, and 72 h and analyzed with a CCK-8 assay. (B,C) The cells were treated with IL-1β (10 ng/mL) with or without SsBb (1, 5, and 10 μg/mL). The protein expression levels of iNOS, COX-2, and IL-6 were determined using Western blotting. (D) q-PCR was used to determine the mRNA levels of iNOS, COX-2, and IL-6. Data are presented as the mean ± SEM of three independent experiments. *p < 0.05, **p < 0.01, ***p < 0.001; ns, no significance.

effects of the three groups of different concentrations. Therefore, according to the principle of drug dosage minimization, 1 μg/mL was chosen for the subsequent experiments.

2.5. SsBb Inhibits Inflammation by the NF-κB Pathway in Chondrocytes. We explored the pathways by which SsBb inhibits inflammation in chondrocytes using RNA-Seq of human chondrocytes from the control, IL-1β, and SsBb groups. To thoroughly investigate the potential pathways involved in the inflammatory responses, Fisher's exact test was employed for KEGG pathway analysis of these differentially expressed genes (DEGs). The KEGG analysis showed that 39 KEGG pathways were significantly enriched for these DEGs (P < 0.05), which mainly participated in pathways linked to the inflammatory pathways, immune system, and infectious diseases. The NF-κB signaling pathway is significant in the immune- and inflammation-associated pathways (Figures S1 and S2). Based on the results of RNA-Seq, we examined the NF-κB signaling pathway. It has been shown that the NF-κB pathway is an important signaling pathway in the inflammatory response. Therefore, we used Western blotting to analyze the phosphorylation levels of p65 and iKBa. As shown in Figure S3, SsBb-treated chondrocytes inhibited IL-1β-induced phosphorylation of p65 and iKBa.

2.6. Biological Properties of the SsBb/GelMA Hydrogel. To test the toxicity of GelMA and SsBb/GelMA hydrogels for cells, live/dead staining kits were used (Figure 4A,B). At 1 day of culture, most of the chondrocytes within the hydrogel had a round or pike shape morphology. The cells began to stretch and proliferate with time, and dead cells were very rare. There was no significant difference in cell adhesion or proliferation within the hydrogel between both groups.

https://doi.org/10.1021/acsomega.4c07489
ACS Omega 2024, 9, 49597−49608

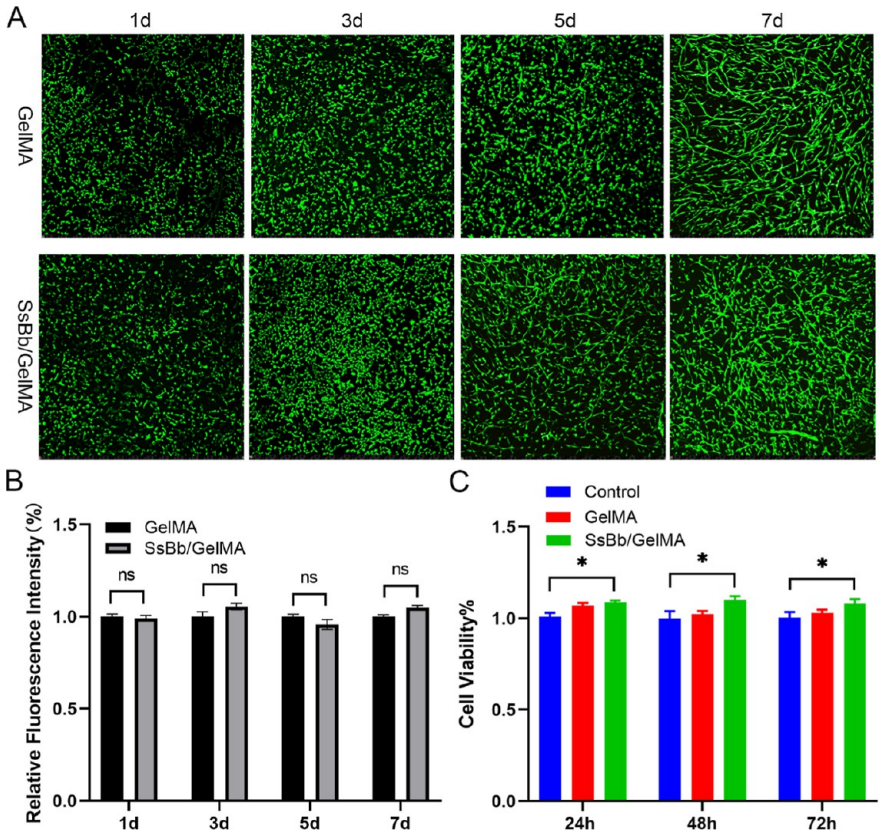

Figure 4. Biological properties of the SsBb/GelMA hydrogel. (A) GelMA and SsBb/GelMA groups were stained by live/dead fluorescent staining. (B) Relative fluorescence intensity of GelMA and SsBb/GelMA groups. (C) Cytotoxicity of GelMA and SsBb/GelMA hydrogels in human chondrocytes (24, 48, and 72 h). *$p < 0.05$; ns, no significance.

To detect cell proliferation on GelMA and SsBb/GelMA hydrogels, the CCK-8 reagent was used. As shown in Figure 4C, cells cultured with GelMA and SsBb/GelMA hydrogel leaching solution showed good cell viability within 72 h and did not show a significant difference from the control.

2.7. In Vitro Inflammation Inhibition by the SsBb/GelMA Hydrogel. Western blot and q-PCR were used to detect the anti-inflammatory effects of SsBb/GelMA hydrogels in vitro. The treatment of SsBb decreased the levels of inflammation-related proteins, including iNOS, COX-2, and IL-6, which were increased by IL-1β (Figure 5A−D). And the q-PCR results were consistent with the results of Western blot experiments (Figure 5E−G).

2.8. In Vivo Inflammatory Response by Histological and Immunohistochemical Staining. We assessed the inflammatory response around the hydrogel after 2 w, 4 w, and 8 w of implantation. Hematoxylin−eosin (H&E) staining results confirmed that both groups of hydrogels showed inflammatory response at the implant−host interface at 2 weeks (Figure 6B). However, the inflammatory reaction around the SsBb/GelMA hydrogels was significantly reduced at 4 and 8 weeks.

Toluidine blue staining was used to assess chondrogenically differentiated cells and cartilaginous tissue maturity and quality. The background of the tissue sections was blue, while the cartilage area was purple-red. As shown in Figure 6C, both groups of hydrogels showed no visible cartilage tissue formation at 2 weeks and began to show cartilage formation at 4 weeks. It is noteworthy that the SsBb/GelMA hydrogels showed more areas of positive staining at both 4 and 8 weeks. This suggests that SsBb/GelMA hydrogel implants have higher quality and a more stable cartilage formation.

Masson staining was used to assess the thickness of the collagenous envelope around the hydrogel implants. As shown in Figure 7A, both hydrogel implants were surrounded by a layer of inflammatory cells at the hydrogel−host tissue interface. The collagen thickness at the SsBb/GelMA hydrogel−tissue interface was significantly lower than that of the GelMA hydrogel (Figure 7B−D).

Expression of the inflammatory cytokine IL-6 was detected by immunohistochemistry (Figure 8A). Compared with the GelMA hydrogel group, the SsBb/GelMA hydrogel group exhibited lower IL-6 expression at all times of implantation, with significant differences (Figure 8B−D).

3. DISCUSSION

The immune-inflammatory response after biomaterial implantation has been reported to be an important factor hindering tissue repair and regeneration.[26,27] However, anti-inflammatory biomaterials have not been fully developed.[28] In this study, the anti-inflammatory effect of SsBb on chondrocytes was first recognized. Not only that, the SsBb/GelMA hydrogel also had anti-inflammatory effects and modulated the inflammatory response generated at the early stage of biomaterial implantation.

Soyasaponins are amphiphilic oleanoid triterpenoid glycosides with a variety of health-promoting bioactivities.[29] Soyasaponins have been documented to have a regulatory effect on macrophages, inhibiting prostaglandin E2 (PGE2), nitric oxide (NO), and TNF-a and decreasing the mRNA

https://doi.org/10.1021/acsomega.4c07489
ACS Omega 2024, 9, 49597−49608

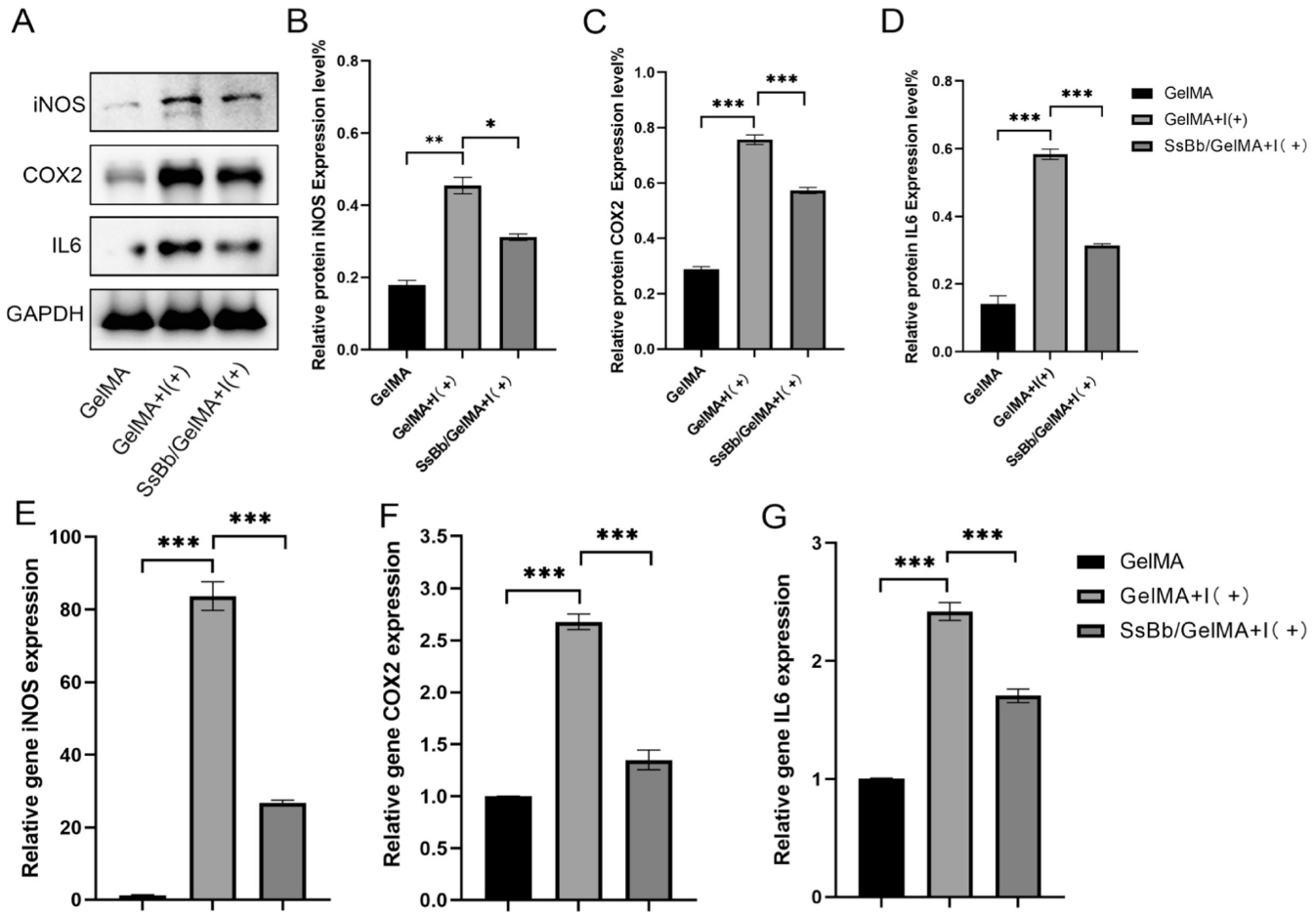

Figure 5. SsBb/GelMA's protective effects against inflammation induced by IL-1β. (A–D) The protein expression levels of iNOS, COX-2, and IL-6 were determined using Western blotting. (E–G) q-PCR was used to determine the mRNA levels of iNOS, COX-2, and IL-6. *p < 0.05, **p < 0.01, ***p < 0.001. I (+), IL-1β.

expression levels of cyclooxygenase (COX-2) and inducible nitric oxide (NO) synthase in LPS-activated peritoneal macrophages.[30] In addition to this, IL-6 released by M1 macrophages has an important role in early acute inflammation.[31,32] In the experimental results of this study, we can see that SsBb played an ameliorative role in the IL-1β-induced chondrocyte inflammation model, reducing the protein and mRNA expression levels of iNOS, COX-2, and IL-6. It is worth mentioning that although all three concentrations of SsBb showed significant ameliorative effects on the chondrocyte inflammation model, there was no significant difference among the three groups. Therefore, according to the principle of the minimum effective dose,[33] 1 μg/mL of SsBb was chosen for the subsequent experiments, which was also more favorable for clinical translation.

Among the many pathways associated with the inflammatory response, the NF-κB signaling pathway is important.[34,35] IKK signaling-induced phosphorylation of the IκB molecule, on the other hand, is a central event in the activation of the NF-κB signaling pathway.[36] IKKβ is essential for typical NF-κB activation by proinflammatory cytokines and a variety of microbial products. Activated IKKβ induces the phosphorylation of IκB proteins, leading to K48-linked ubiquitylation of IκBs and their subsequent degradation, which subsequently results in the release of the NF-κB dimer from cytoplasmic inhibition.[37] The released NF-κB dimers translocate to the nucleus and drive transcription of target genes.[38] We analyzed the mechanisms involved in the inhibition of inflammatory responses by SsBb by RNA-seq and confirmed that the NF-κB signaling pathway is closely related to this study. Our results also showed that IL-1β-induced inflammatory response activated the NF-κB signaling pathway. However, SsBb reversed this situation by inhibiting the phosphorylation of p65 and iKBa, thus reducing the expression of inflammation-related markers in chondrocytes.

GelMA, as an ideal biomaterial, has a cross-linked three-dimensional porous structure that closely resembles some of the basic properties of ECM.[39] This is due to the presence of cell attachment and matrix metalloproteinase-responsive peptide motifs in GelMA, which allows cells to proliferate and spread in the scaffold of GelMA.[40] It is worth noting that chemical modification of gelatin by MA generally involves less than a 5% molar ratio of amino acid residues, which means that most of the functional amino acid motifs (RGD motifs and MMP-degradable motifs) are not significantly affected.[41] The arginine–glycine–aspartate acid (RGD) sequence promotes cell attachment, and the matrix metalloproteinase (MMP) target sequence is suitable for cell remodeling. During the configuration of GelMA solutions, the mass/volume fraction is typically 5% w/v to 30% w/v. The mass/volume fraction influences the biological properties of GelMA hydrogels.[42] In general, the mass/volume fraction is proportional to the mechanical strength of the hydrogel and inversely proportional to the swelling rate and cell proliferation.[43] And the swelling

https://doi.org/10.1021/acsomega.4c07489
ACS Omega 2024, 9, 49597–49608

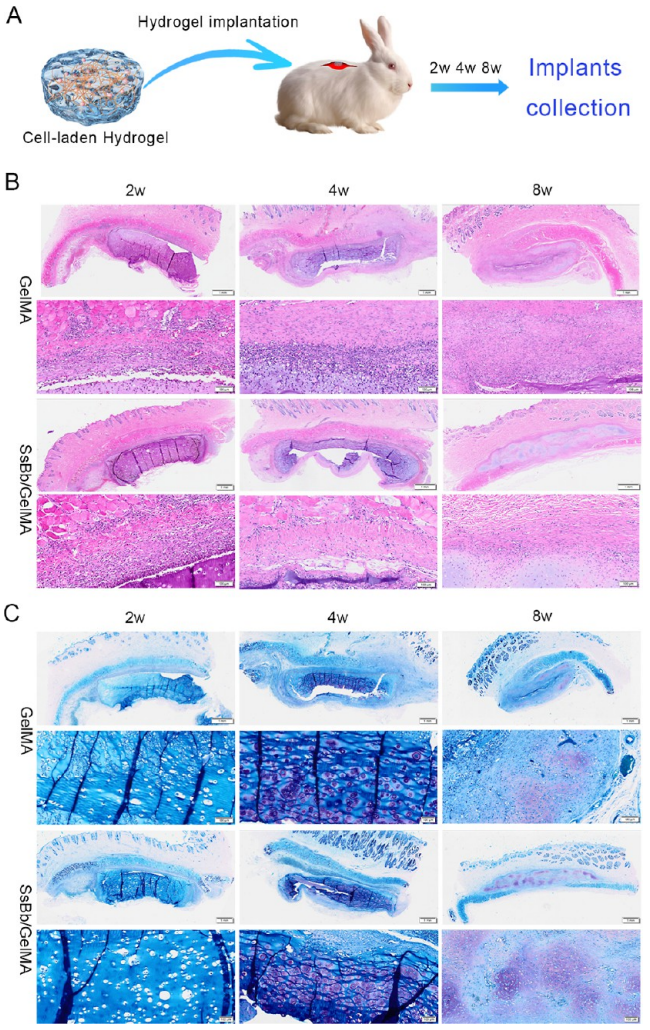

Figure 6. In vivo histological comparison of hydrogels implanted into the back of rabbits. (A) In vivo implantation and removal of the hydrogel. (B) Peri-implant inflammatory response assessed by H&E staining results at 2, 4, and 8 weeks after in vivo implantation of GelMA and SsBb/GelMA groups. (C) The cartilaginous tissue maturity and quality of hydrogels after in vivo implantation at 2, 4, and 8 weeks.

property of hydrogel represents the water absorption property as well as the space to accommodate the cells.[30] Therefore, the 10% (w/v) GelMA hydrogel was chosen for this study. GelMA also acted as a drug carrier and was successfully loaded with SsBb. There was no explosive drug release from SsBb/GelMA but rather a slow, steady, and long-lasting release. The alteration of the chemical bond occurs during physical blending and UV cross-linking of SsBb and GelMA. As a result, the pore size of SsBb/GelMA hydrogels decreased while the mechanical strength was enhanced. However, the reduced pore size did not affect the biological properties of SsBb/GelMA, as determined by in vitro live/dead staining results and anti-FBR response tests.

Moreover, the anti-inflammatory effect of the SsBb/GelMA hydrogel was significantly better than that of the pure GelMA hydrogel, which was consistent with the previous expectation. The experimental results of immunohistochemical staining also showed that the SsBb/GelMA hydrogel had the same anti-FBR effect in vivo. At 2 weeks of implantation, there was a clear, dense inflammatory cell enrichment of the SsBb/GelMA hydrogel at the implant−host interface, albeit in a very thin layer, but this phenomenon subsequently disappeared at 4 and 8 weeks. This occurrence may be due to the slow release of the drug from SsBb. However, this did not affect the proliferation and differentiation of chondrocytes within the SsBb/GelMA hydrogel or the maintenance of the phenotype. The biochemistry and specific mechanism of action of the compound soyasaponin are also worth exploring. Since the activation of the NF-kB may affect ROS production, the role of free radicals and ROS in the context of inflammation and tissue engineering needs to be explored. The mechanism of NF-kB activation during inflammatory responses and its subsequent effects on ROS production can be studied. Besides, the effect of elevated ROS on chondrocyte viability, proliferation, and differentiation, as well as their implications for the integration of tissue engineering implants, is also a direction. Antioxidants or other approaches should be investigated to mitigate ROS production and improve tissue integration.

In summary, soyasaponin Bb, as a small molecule in traditional Chinese medicine, can regulate the inflammatory response of chondrocytes induced by IL-1β and inhibit the expression of inflammation-related markers. Multiple signaling pathways were found to be related to the anti-inflammatory effects of SsBb by RNA-Seq results, while the NF-κB signaling pathway was selected, which confirmed its role in the inhibition of inflammatory responses by SsBb. SsBb/GelMA, as a new direction for anti-FBR biomaterials, can alleviate the foreign body reaction after hydrogel implantation and help stabilize the repair and regeneration of cartilage tissue. We believe that SsBb/GelMA hydrogels have potential applications in the development of anti-FBR biomaterials and tissue regeneration and repair.

4. CONCLUSIONS

In summary, we confirmed that SsBb has the ability to inhibit the inflammatory response of chondrocytes, which is achieved through the NF-κB signaling pathway. Not only that, we also developed SsBb/GelMA hydrogel scaffolds capable of stable drug release, with the ability of anti-FBR and stable tissue repair and regeneration. As an anti-FBR biomaterial, the SsBb/GelMA hydrogel has the potential not only for cartilage tissue repair but also can be equally developed for other tissue repair or wound healing processes related to inflammatory response.

5. MATERIALS AND METHODS

5.1. Chemicals and Reagents. Soyasaponin Bb (MCE, China). GelMA (EFL, China). IL-1β (MCE, China). Cell Counting Kit-8 (Invitrogen, America). Anti-GAPDH antibody (60004-1-Ig, Proteintech, China). Anti-iNOS antibody (18985-1-AP, Proteintech, China). Anti-COX2 antibody (12375-1-AP, Proteintech, China). Anti-IL6 antibody (21865-1-AP, Proteintech, China). Anti-p65 antibody (10745-1-AP, Proteintech, China). Anti-pp65 (3033S, CST, China). Anti-ikBa antibody (10268-1-AP, Proteintech, China). Anti-pikBa antibody (2859S, CST, China). Anti-Histone H3 antibody (17168-1-AP, Proteintech, China).

5.2. Fabrication of the SsBb/GelMA Hydrogel. GelMA was purchased from EFL (China). Briefly, SsBb powder was first dissolved with complete medium at a concentration of 0.1 mg/mL. The 10% GelMA hydrogel was configured by dissolving 1 g of GelMA with 10 mL of photoinitiator (LAP) (0.25% w/v) at 60 °C, followed by bacterial filtration

https://doi.org/10.1021/acsomega.4c07489
ACS Omega 2024, 9, 49597−49608

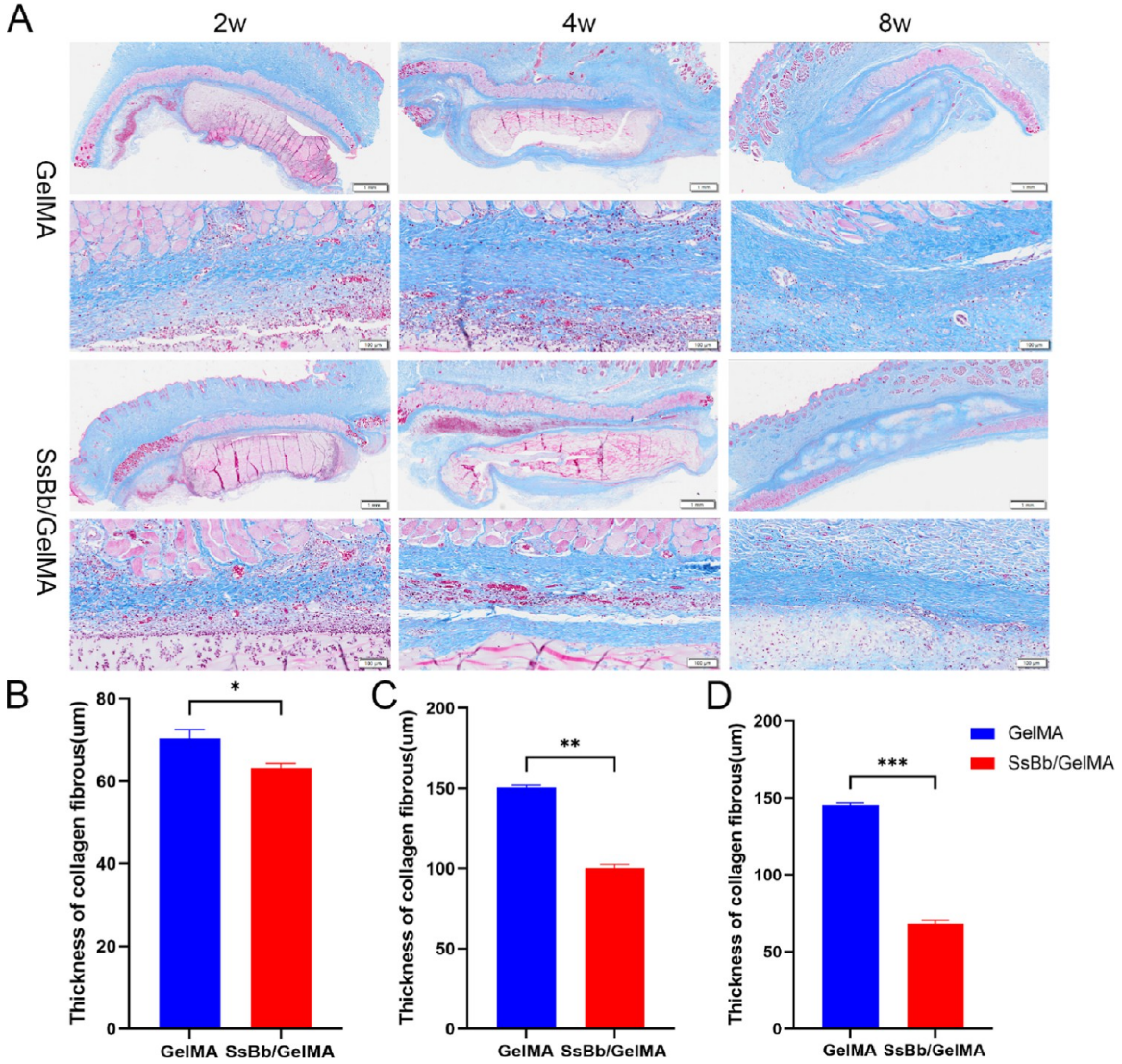

Figure 7. In vivo collagen thickness by Masson staining. (A) The Masson results of GelMA and SsBb/GelMA hydrogels after in vivo implantation at 2, 4, and 8 weeks. (B–D) The thickness of collagen fibrous tissue at 2, 4, and 8 weeks. *$p < 0.05$, **$p < 0.01$, ***$p < 0.001$.

with a 0.22 μm filter. The SsBb solution was physically co-mixed with the GelMA solution at room temperature with sufficient stirring to configure a SsBb/GelMA hydrogel, which was subsequently cross-linked to form a cylindrical hydrogel with a diameter of 8 mm and a height of 2 mm under 405 nm UV illumination and stored at 4 °C.

5.3. Drug Release of the SsBb/GelMA Hydrogel. The hydrogel sample was immersed in 10 mL of PBS buffer solution (pH 7.4, 0.01 M) and placed at 37 °C, and the same amount of sample was collected at predetermined intervals and added to a certain volume of fresh buffer solution media to maintain the simulated release conditions. The concentration of SsBb was then determined by using HPLC analysis (Waters2695). The mobile phase consisted of acetonitrile (solvent A), water (solvent B), and acetonitrile at a flow rate of 1.0 mL/min. The chromatographic column used was Ultimate SHISEIDO PAK C18 ACR (4.6 mm × 250 mm, 5 μm); the wavelength detector was set to 203 nm. The samples of each experiment were analyzed in triplicate. The cumulative release percentage was calculated for each time point interval.

5.4. Surface Morphology of the SsBb/GelMA Hydrogel. GelMA and SsBb/GelMA were immersed in PBS after fully UV cross-linking. The pore structure and size of samples were observed by cryo-SEM (Sigma 300 + Quorum pp3010 + Oxford ULTIM MAX 100). The pictures were randomly selected by cryo-SEM and magnified 400 times and 800 times to observe the surface morphology of the hydrogel at least three times.

5.5. Mechanical Testing of the SsBb/GelMA Hydrogel. In order to characterize the mechanical properties of the hydrogel, GelMA and SsBb/GelMA hydrogels were tested using the equivalence force test instrument. The samples were molded into cylindrical shapes with a diameter of 2 cm and a height of 0.5 cm to test the compress stress. The speed of stretching and compressing is 1 mm/min. The stress–strain curves were drawn after three random tests.

5.6. Swelling and Degradation Characteristics of SsBb/GelMA. Each sample was immersed in 1 mL of double-distilled water at a constant temperature of 37 °C to verify the swelling behavior of hydrogels ($n = 3$). In order to test the swelling rate of hydrogels, samples were removed to record wet weight (W_t) and measured within 1 day of collection. Each hydrogel was weighed before immersion and recorded as W_0. The swelling rate was calculated using the

https://doi.org/10.1021/acsomega.4c07489
ACS Omega 2024, 9, 49597–49608

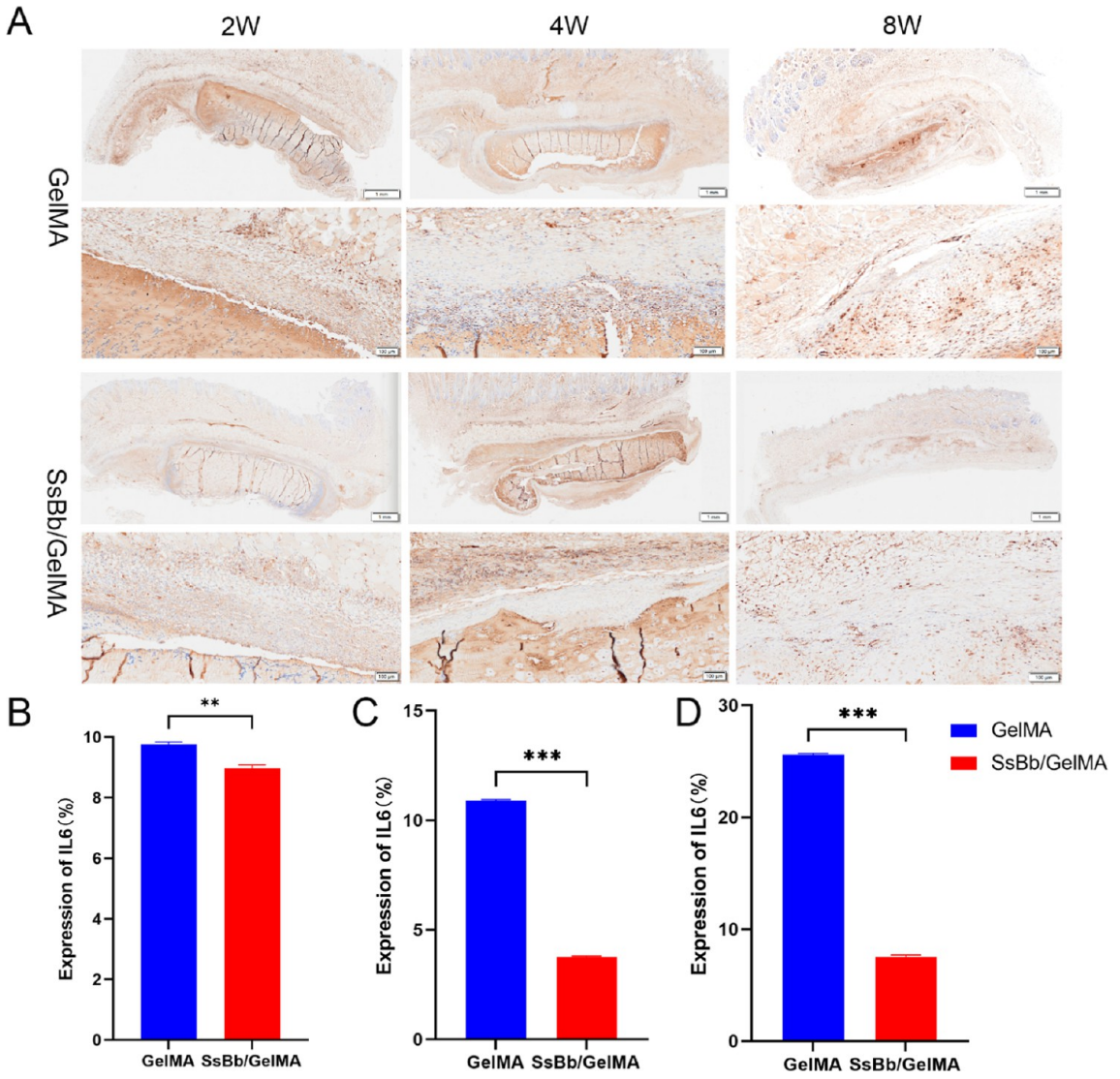

Figure 8. In vivo immunohistochemistry for IL-6. (A) The immunohistochemistry for IL-6 results of GelMA and SsBb/GelMA hydrogels after in vivo implantation at 2, 4, and 8 weeks. (B–D) The percentage of the expression of IL-6 with immunohistochemistry. $^{**}p < 0.01$, $^{***}p < 0.001$.

following equation: $S\ \% = (W_t - W_0)/W_0 \times 100\%$. Each group measured three parallel specimens.

In order to test the degradation rate of hydrogels, samples were removed to record the original weight (W_0). Each sample was immersed in 1 mL of double-distilled water at a constant temperature of 37 °C and weighed every 7 days after lyophilizing for 24 h according to the time point. The dry weight of the samples was calculated as W_1. Then, the hydrogel degradation rate was calculated using the following equation: $E\ \% = (W_0 - W_1)/W_0 \times 100\%$. Each group measured three parallel specimens.

5.7. Fourier Infrared Spectroscopy of GelMA and SsBb/GelMA. The chemical properties of the hydrogels photo-cross-linked were characterized by Fourier transform infrared spectroscopy (FTIR). Data acquisition was performed using an FTIR spectrometer (Varian 670, Agilent, Santa Clara, CA, USA) connected to a plotting microscope (Varian 620-IR, Agilent, Santa Clara, CA, USA). Obtained samples were analyzed in the interval from 400 to 4000 cm^{-1} with a spectral resolution of 4 cm^{-1} with 64 scans per minute and a total of 100 scans per spectrum.

5.8. Primary Cell Extraction and Culture. The acquisition of human auricular cartilage specimens was approved by the Ethics Committee of The First Hospital of Jilin University, and animal experiments were both approved by the Ethics Committee of Jilin University. Microtia ear cartilage specimens were obtained during the third stage of ear reconstructive surgery, which is to reshape the implanted scaffold by getting rid of redundant cartilage. Specimens were carefully dissected to remove the fibrous tissue. Chondrocytes were isolated by digesting minced cartilage tissue ($1 \times 2\ cm^2$) with collagenase II (0.2%; Biosharp, China) for 6 h at 37 °C with gentle agitation.[44] The suspension was filtered through a nylon mesh (200 μm) followed by centrifugation at 1000 rpm for 10 min, and the cells were harvested, counted, and plated at a density of 1.5×10^4 cells/cm^2 for culture in the regular media [Dulbecco's modified Eagle's medium (DMEM), 10% fetal bovine serum (FBS), 100 U/mL penicillin, and 0.1 mg/mL streptomycin] in a humidified 37 °C incubator with 5% CO_2. To prevent phenotypic loss, we used only the P2 chondrocytes.[44]

5.9. Cell Experiments. The P2 chondrocytes were made into 3×10^4/mL cell suspension, inoculated in 96-well plates,

https://doi.org/10.1021/acsomega.4c07489
ACS Omega 2024, 9, 49597−49608

100 μL per well, after 24 h of wall affixation, different concentrations of SsBb (1−100 μg/mL) were added for grouping, 10 μL of CCK8 assays was added to each well after 24, 48, and 72 h of intervention, and then the cells were incubated in the incubator for 2.5 h and then detected. The cell viability of each group was calculated according to the formula to screen the optimal concentration of SsBb on chondrocytes. The concentrations of SsBb in chondrocytes were 1, 5, and 10 μg/mL. IL-1β was used to induce the chondrocyte inflammation model at 10 ng/mL.[45] The endotoxin test was performed prior to implants using the chromogenic LAL endotoxin assay kit (Beyotime, China).

5.10. Western Blot. To test changes in chondrocyte inflammation-related proteins, expression of iNOS, COX-2, IL-6, GADPH, iKBa, p-iKBa, p65, p-p65, and Histone3 was examined. Appropriate amounts of RIPA lysis buffer and protease inhibitor were used to dissolve the cells. The concentration of the total protein was determined by the BCA method. 50 μg of total protein was electrophoresed on a 10% SDS-PAGE gel, electrolyzed to nitrocellulose membrane, blocked with skim milk for 1 h, and incubated with primary antibody (1:1000) at 4 °C overnight, fully washed, and incubated with HRP-labeled secondary antibody (1:5000) for 1 h at room temperature. Finally, ECL reagents were added to obtain the band, and the Image Pro image analysis software was used to scan the gray values of each band. The GAPDH and Histone3 protein levels were used as an internal reference.

5.11. q-PCR. Total RNA was isolated from human chondrocytes using the TRIzol reagent (Invitrogen, Carlsbad, CA, USA). RNA concentrations were detected and adjusted to the same concentrations before reverse transcription with the PrimeScript RT Master Mix (TransGen, Biotech). SYBR Premix Ex *Taq*II (TransGen, Biotech) and the 7500 real-time PCR system (7500, Applied Biosystems, USA) were used for q-PCR. Briefly, the final PCR system was carried out in a 20 μL system in the following procedure: initial denaturation (95 °C, 5 min), then subjected to 40 cycles of denaturation (95 °C, 10 s), annealing, and extension (60 °C, 30 s). The sequence information for each primer used for gene expression analysis was as follows: COX2, F 5′CTGGCGCTCAGCCATACAG R 5′CGCACTTATACTGGTCAAATCCC; iNOS, F 5′TTCSGTATCACAACCTCAGCAAG R 5′TGGACCTGCAAGTTAAAATCCC; IL-6, F 5′ACTCACCTCTTCAGAACGAATTG R 5′CCATCTTTGGAAGGTTCAGGTTG; and GAPDH, F 5′GGAGCGAGATCCCTCCAAAAT R 5′GGCTGTTGTCATACTTCTCATGG. The amplification efficiency and specificity of the primers have been validated. Gene expression was analyzed for fold differences using $2^{-\Delta\Delta CT}$ with GAPDH as the internal reference control.

5.12. RNA-Seq. Total RNA was extracted from the chondrocytes using the TRIzol reagent as before. RNA samples were detected based on the A260/A280 absorbance ratio with a Nanodrop ND-2000 system (Thermo Scientific, USA), and the RIN of RNA was determined by an Agilent Bioanalyzer 4150 system (Agilent Technologies, CA, USA). Only qualified samples were used for library construction. Paired-end libraries were prepared using a mRNA-seq Lib Prep kit (ABclonal, China) following the manufacturer's instructions. Sequencing was performed with an Illumina NovaSeq 6000/MGISEQ-T7 instrument. The data generated from the Illumina/BGI platform were used for bioinformatics analysis. All of the analyses were performed by using an in-house pipeline from Shanghai Applied Protein Technology. Then, clean reads were separately aligned to the reference genome with orientation mode using HISAT2 software (http://daehwankimlab.github.io/hisat2/) to obtain mapped reads. Feature Counts (http://subread.sourceforge.net/) was used to count the read numbers mapped to each gene. And then, FPKM of each gene was calculated based on the length of the gene and read count mapped to this gene. Moreover, differential expression analysis was performed using DESeq2 (http://bioconductor.org/packages/release/bioc/html/DESeq2.html); DEGs with |log2 FC| > 1 and $P_{adj} < 0.05$ were considered to be significantly different expressed genes. We use the clusterProfiler R software package for GO function enrichment and KEGG pathway enrichment analysis. When $P < 0.05$, it is considered that the GO or KEGG function is significantly enriched.

5.13. Culture of Chondrocytes on the SsBb/GelMA Hydrogel. Primary chondrocytes were extracted. The P2 chondrocytes were collected at full growth and made into cell precipitates, which were analyzed with GelMA and SsBb/GelMA solution to resuspend and obtain a cell suspension with a density of 4×10^6/mL. Subsequently, the 125 μL suspension solution was used to prepare a cell-laden hydrogel, as before. The cell-laden hydrogels were placed in 12-well plates and incubated in DMEM at 37 °C, 5% CO_2, and the medium was changed every 2 days.

5.14. Cell Proliferation Assay. In order to measure the proliferation of cells on hydrogel materials, a cell counting kit-8 (CCK8) was used. Briefly, a leaching solution was prepared by soaking GelMA and SsBb/GelMA hydrogels in HIGH DMEM for 3 days. The P2 chondrocytes were made into a 3×10^4/mL cell suspension, inoculated in 96-well plates, 100 μL per well, with 6 wells per group, and the plate was incubated in a 5% CO_2 constant temperature incubator at 37 °C for 24 h. The culture medium was then replaced with a leaching solution. After culturing for another 24, 48, and 72 h, 10 μL of CCK8 solution was added to each well and incubated for 2.5 h. The wells subsequently were detected using an immunoenzyme-labeled instrument at a wavelength of 450 nm.

To test the toxicity of SsBb/GelMA hydrogels, samples were placed in 12-well plates. Live-dye dyeing was performed on days 1, 3, 5, and 7, and images of live/dead assays were observed by fluorescence microscopy (ZEISS, Germany) under excitation conditions of 488 and 568. Green fluorescence was used for living cells and a red fluorometer for dead cells, and the number and status of cells were assessed.

5.15. In Vitro Inflammation Inhibition by the SsBb/GelMA Hydrogel. To explore the role of the SsBb/GelMA hydrogel in modulating inflammation in vitro, Western blot and q-PCR were used. First, the cell-laden hydrogels were made as before. After culturing for 7 d, the cell-laden hydrogel samples were washed with PBS three times, and the hydrogels were cleaved with GelMA lysis solution. Subsequently, cellular proteins and RNA were extracted for Western blot and q-PCR.

5.16. Establishment of the Rabbit Model. To detect in vivo inflammatory regulation, cell-laden hydrogel samples were implanted on the backs of rabbits. Briefly, male rabbits aged 4 months were selected, and one ear was taken under isoflurane anesthesia to extract primary chondrocytes of rabbit ear. The rabbit P2 chondrocytes were collected when full-grown and mixed with GelMA and SsBb/GelMA solutions to form a 4×10^6/mL cell suspension, which was subsequently fabricated as cell-laden hydrogel samples for implantation in the back pocket of the same rabbit.[8] After 2, 4, and 8 weeks of incubation, the

https://doi.org/10.1021/acsomega.4c07489
ACS Omega 2024, 9, 49597−49608

samples were taken out for H&E, toluidine blue, Masson, and IL-6 immunohistochemical staining to detect the inflammatory encapsulation response of the implants.

5.17. H&E, Toluidine Blue, Masson, and Immunohistochemical Staining. The samples were thoroughly washed with physiological saline and immersed in 4% paraformaldehyde for 24 h. After dehydrating and wax block embedding, paraffin sectioning was sliced to a thickness of 5 μm to stain.

The sections were subjected to dewaxing pretreatment. H&E staining and toluidine blue staining were carried out for 10 and 30 min, respectively, and the sections were gradually stained according to the Masson kit (Solarbio, China), followed by dehydration of the alcohol gradient, and the resin gel was sealed after air drying.[46] Morphological observations were made at random selection and photographed using an OLYMPUS VS200 slide scanner.

After the dewaxing pretreatment, the sections were gradually stained according to the UltraSensitive SP IHC kit (MXB, China). Sections were incubated with antibodies against IL-6 to observe the expression changes. Immunopositive particles were observed at random selection and photographed using an OLYMPUS VS200 slide scanner.

The histology and IHC were quantified by FIJI ImageJ and GraphPad. The regions were observed at random selection, and 5 fields of view at 40× were selected for each section to be observed. The results were blinded and assessed by two professional pathologists.

5.18. Statistical Analysis. All the data were analyzed with an ANOVA test using GraphPad for Windows. A probability value of $p < 0.05$ was statistically significant. Image statistics were analyzed by ImageJ.

■ ASSOCIATED CONTENT

Supporting Information

The Supporting Information is available free of charge at https://pubs.acs.org/doi/10.1021/acsomega.4c07489.

Main category terms of KEGG analysis; KEGG pathway enrichment analysis; and SsBb inhibition of the activation of the NF-κB signaling pathway (PDF)

■ AUTHOR INFORMATION

Corresponding Authors

Tian Li − *Department of Plastic and Reconstructive Surgery, The First Hospital of Jilin University, Changchun 130021, P. R. China;* orcid.org/0000-0003-3578-6464; Email: litian@jlu.edu.cn

Duo Zhang − *Department of Plastic and Reconstructive Surgery, The First Hospital of Jilin University, Changchun 130021, P. R. China;* orcid.org/0000-0002-7372-6799; Email: zhangduo@jlu.edu.cn

Authors

Yuhan Jiang − *Department of Plastic and Reconstructive Surgery, The First Hospital of Jilin University, Changchun 130021, P. R. China*

Tenghai Li − *Department of Plastic and Reconstructive Surgery, The First Hospital of Jilin University, Changchun 130021, P. R. China*

Bingzhang Liu − *Department of Plastic and Reconstructive Surgery, The First Hospital of Jilin University, Changchun 130021, P. R. China*

Yufeng Tian − *Department of Plastic and Reconstructive Surgery, The First Hospital of Jilin University, Changchun 130021, P. R. China*

Yixin Wang − *Department of Plastic and Reconstructive Surgery, The First Hospital of Jilin University, Changchun 130021, P. R. China*

Complete contact information is available at: https://pubs.acs.org/10.1021/acsomega.4c07489

Author Contributions

Duo Zhang and Tian Li: conceptualization; Yuhan Jiang: writing—original draft; Tenghai Li: supervision; Bingzhang Liu: software; Yufeng Tian and Yixin Wang: resources.

Notes

The authors declare no competing financial interest.

■ ACKNOWLEDGMENTS

This work was supported by the projects from CAMS Innovation Fund for Medical Sciences [Grant Number: CAMS-2017-I2M-1-007], The First Hospital of Jilin University [Grant Number: 0404694001], and Jilin Provincial Science-technologic Department [Grant Number: YDZJ202301-ZYTS443].

■ REFERENCES

(1) Huey, D. J.; Hu, J. C.; Athanasiou, K. A. Unlike bone, cartilage regeneration remains elusive. *Science* **2012**, *338* (6109), 917−921.

(2) Harris, J. D.; Siston, R. A.; Pan, X.; Flanigan, D. C. Autologous chondrocyte implantation: a systematic review. *J. Bone Jt. Surg., Am. Vol.* **2010**, *92* (12), 2220−2233.

(3) Peterson, L.; Vasiliadis, H. S.; Brittberg, M.; Lindahl, A. Autologous chondrocyte implantation: a long-term follow-up. *Am. J. Sports Med.* **2010**, *38* (6), 1117−1124.

(4) Benazzo, F.; Cadossi, M.; Cavani, F.; Fini, M.; Giavaresi, G.; Setti, S.; Cadossi, R.; Giardino, R. Cartilage repair with osteochondral autografts in sheep: effect of biophysical stimulation with pulsed electromagnetic fields. *J. Orthop. Res.* **2008**, *26* (5), 631−642.

(5) Raikin, S. M. Fresh osteochondral allografts for large-volume cystic osteochondral defects of the talus. *J. Bone Jt. Surg., Am. Vol.* **2009**, *91* (12), 2818−2826.

(6) Haene, R.; Qamirani, E.; Story, R. A.; Pinsker, E.; Daniels, T. R. Intermediate outcomes of fresh talar osteochondral allografts for treatment of large osteochondral lesions of the talus. *J. Bone Jt. Surg., Am. Vol.* **2012**, *94* (12), 1105−1110.

(7) Kwon, H.; Brown, W. E.; Lee, C. A.; Wang, D.; Paschos, N.; Hu, J. C.; Athanasiou, K. A. Surgical and tissue engineering strategies for articular cartilage and meniscus repair. *Nat. Rev. Rheumatol.* **2019**, *15* (9), 550−570.

(8) Zhang, D.; Chen, Q.; Bi, Y.; Zhang, H.; Chen, M.; Wan, J.; Shi, C.; Zhang, W.; Zhang, J.; Qiao, Z.; et al. Bio-inspired poly-DL-serine materials resist the foreign-body response. *Nat. Commun.* **2021**, *12* (1), 5327.

(9) Anderson, J. M. Multinucleated giant cells. *Curr. Opin. Hematol.* **2000**, *7* (1), 40−47.

(10) Gretzer, C.; Emanuelsson, L.; Liljensten, E.; Thomsen, P. The inflammatory cell influx and cytokines changes during transition from acute inflammation to fibrous repair around implanted materials. *J. Biomater. Sci. Polym. Ed.* **2006**, *17* (6), 669−687.

(11) Luttikhuizen, D. T.; Harmsen, M. C.; Luyn, M. J. V. Cellular and molecular dynamics in the foreign body reaction. *Tissue Eng.* **2006**, *12* (7), 1955−1970.

(12) Martin, K. E.; García, A. J. Macrophage phenotypes in tissue repair and the foreign body response: Implications for biomaterial-based regenerative medicine strategies. *Acta Biomater.* **2021**, *133*, 4−16.

(13) Cegielski, M.; Izykowska, I.; Podhorska-Okolow, M.; Zabel, M.; Dziegiel, P. Development of foreign body giant cells in response to implantation of Spongostan as a scaffold for cartilage tissue engineering. *In Vivo* **2008**, *22* (2), 203−206.
(14) Eslami-Kaliji, F.; Hedayat Nia, N.; Lakey, J. R. T.; Smink, A. M.; Mohammadi, M. Mechanisms of Foreign Body Giant Cell Formation in Response to Implantable Biomaterials. *Polymers* **2023**, *15* (5), 1313.
(15) Taraballi, F.; Sushnitha, M.; Tsao, C.; Bauza, G.; Liverani, C.; Shi, A.; Tasciotti, E. Biomimetic Tissue Engineering: Tuning the Immune and Inflammatory Response to Implantable Biomaterials. *Adv. Healthcare Mater.* **2018**, *7* (17), No. e1800490.
(16) Kass, L. E.; Nguyen, J. Nanocarrier-hydrogel composite delivery systems for precision drug release. *Wiley Interdiscip. Rev.: Nanomed. Nanobiotechnol.* **2022**, *14* (2), No. e1756.
(17) Qian, C.; Zhang, T.; Gravesande, J.; Baysah, C.; Song, X.; Xing, J. Injectable and self-healing polysaccharide-based hydrogel for pH-responsive drug release. *Int. J. Biol. Macromol.* **2019**, *123*, 140−148.
(18) Zhang, F.; Scull, G.; Gluck, J. M.; Brown, A. C.; King, M. W. Effects of sterilization methods on gelatin methacryloyl hydrogel properties and macrophage gene expressionin vitro. *Biomed. Mater.* **2023**, *18* (1), 015015.
(19) Isaeva, E. V.; Kisel, A. A.; Beketov, E. E.; Demyashkin, G. A.; Yakovleva, N. D.; Lagoda, T. S.; Arguchinskaya, N. V.; Baranovsky, D. S.; Ivanov, S. A.; Shegay, P. V.; et al. Effect of Collagen and GelMA on Preservation of the Costal Chondrocytes' Phenotype in a Scaffold in vivo. *Sovrem Tekhnologii Med.* **2023**, *15* (2), 5−16.
(20) Zha, L. Y.; Mao, L. M.; Lu, X. C.; Deng, H.; Ye, J. F.; Chu, X. W.; Sun, S. X.; Luo, H. J. Anti-inflammatory effect of soyasaponins through suppressing nitric oxide production in LPS-stimulated RAW 264.7 cells by attenuation of NF-κB-mediated nitric oxide synthase expression. *Bioorg. Med. Chem. Lett.* **2011**, *21* (8), 2415−2418.
(21) Xie, Q.; Gu, X.; Chen, J.; Liu, M.; Xiong, F.; Wu, X.; Zhang, Y.; Chen, F.; Chen, H.; Li, M.; et al. Soyasaponins Reduce Inflammation and Improve Serum Lipid Profiles and Glucose Homeostasis in High Fat Diet-Induced Obese Mice. *Mol. Nutr. Food Res.* **2018**, *62* (19), No. e1800205.
(22) Chen, J.; Ullah, H.; Zheng, Z.; Gu, X.; Su, C.; Xiao, L.; Wu, X.; Xiong, F.; Li, Q.; Zha, L. Soyasaponins reduce inflammation by downregulating MyD88 expression and suppressing the recruitments of TLR4 and MyD88 into lipid rafts. *BMC Complementary Med. Ther.* **2020**, *20* (1), 167.
(23) Fußbroich, D.; Schubert, R.; Schneider, P.; Zielen, S.; Beermann, C. Impact of soyasaponin I on TLR2 and TLR4 induced inflammation in the MUTZ-3-cell model. *Food Funct.* **2015**, *6* (3), 1001−1010.
(24) Zha, L.; Chen, J.; Sun, S.; Mao, L.; Chu, X.; Deng, H.; Cai, J.; Li, X.; Liu, Z.; Cao, W. Soyasaponins can blunt inflammation by inhibiting the reactive oxygen species-mediated activation of PI3K/Akt/NF-kB pathway. *PLoS One* **2014**, *9* (9), No. e107655.
(25) Behranvand, N.; Nasri, F.; Zolfaghari Emameh, R.; Khani, P.; Hosseini, A.; Garssen, J.; Falak, R. Chemotherapy: a double-edged sword in cancer treatment. *Cancer Immunol. Immunother.* **2022**, *71* (3), 507−526.
(26) Zhou, G.; Groth, T. Host Responses to Biomaterials and Anti-Inflammatory Design-a Brief Review. *Macromol. Biosci.* **2018**, *18* (8), No. e1800112.
(27) Yanez, M.; Blanchette, J.; Jabbarzadeh, E. Modulation of Inflammatory Response to Implanted Biomaterials Using Natural Compounds. *Curr. Pharm. Des.* **2018**, *23* (41), 6347−6357.
(28) Velnar, T.; Bunc, G.; Klobucar, R.; Gradisnik, L. Biomaterials and host versus graft response: a short review. *Bosn. J. Basic Med. Sci.* **2015**, *16* (2), 82−90.
(29) Luo, H.; Chen, J.; Su, C.; Zha, L. Advances in the Bioactivities of Phytochemical Saponins in the Prevention and Treatment of Atherosclerosis. *Nutrients* **2022**, *14* (23), 4998.
(30) Chen, P.; Xia, C.; Mei, S.; Wang, J.; Shan, Z.; Lin, X.; Fan, S. Intra-articular delivery of sinomenium encapsulated by chitosan microspheres and photo-crosslinked GelMA hydrogel ameliorates osteoarthritis by effectively regulating autophagy. *Biomaterials* **2016**, *81*, 1−13.
(31) Ehrlich, L. A.; Roodman, G. D. The role of immune cells and inflammatory cytokines in Paget's disease and multiple myeloma. *Immunol. Rev.* **2005**, *208*, 252−266.
(32) Tanaka, T.; Narazaki, M.; Kishimoto, T. Interleukin (IL-6) Immunotherapy. *Cold Spring Harbor Perspect. Biol.* **2018**, *10* (8), a028456.
(33) Otava, M.; Shkedy, Z.; Hothorn, L. A.; Talloen, W.; Gerhard, D.; Kasim, A. Identification of the minimum effective dose for normally distributed data using a Bayesian variable selection approach. *J. Biopharm. Stat.* **2017**, *27* (6), 1073−1088.
(34) Kawai, T.; Akira, S. The role of pattern-recognition receptors in innate immunity: update on Toll-like receptors. *Nat. Immunol.* **2010**, *11* (5), 373−384.
(35) Chen, L. F.; Greene, W. C. Shaping the nuclear action of NF-kappaB. *Nat. Rev. Mol. Cell Biol.* **2004**, *5* (5), 392−401.
(36) Hoffmann, A.; Natoli, G.; Ghosh, G. Transcriptional regulation via the NF-kappaB signaling module. *Oncogene* **2006**, *25* (51), 6706−6716.
(37) Ghosh, S.; Hayden, M. S. New regulators of NF-kappaB in inflammation. *Nat. Rev. Immunol.* **2008**, *8* (11), 837−848.
(38) Wertz, I. E.; Dixit, V. M. Signaling to NF-kappaB: regulation by ubiquitination. *Cold Spring Harbor Perspect. Biol.* **2010**, *2* (3), a003350.
(39) Yue, K.; Trujillo-de Santiago, G.; Alvarez, M. M.; Tamayol, A.; Annabi, N.; Khademhosseini, A. Synthesis, properties, and biomedical applications of gelatin methacryloyl (GelMA) hydrogels. *Biomaterials* **2015**, *73*, 254−271.
(40) Van den Steen, P. E.; Dubois, B.; Nelissen, I.; Rudd, P. M.; Dwek, R. A.; Opdenakker, G. Biochemistry and molecular biology of gelatinase B or matrix metalloproteinase-9 (MMP-9). *Crit. Rev. Biochem. Mol. Biol.* **2002**, *37* (6), 375−536.
(41) Van Den Bulcke, A. I.; Bogdanov, B.; De Rooze, N.; Schacht, E. H.; Cornelissen, M.; Berghmans, H. Structural and rheological properties of methacrylamide modified gelatin hydrogels. *Biomacromolecules* **2000**, *1* (1), 31−38.
(42) Gan, X.; Li, C.; Sun, J.; Zhang, X.; Zhou, M.; Deng, Y.; Xiao, A. GelMA/κ-carrageenan double-network hydrogels with superior mechanics and biocompatibility. *RSC Adv.* **2023**, *13* (3), 1558−1566.
(43) Nichol, J. W.; Koshy, S. T.; Bae, H.; Hwang, C. M.; Yamanlar, S.; Khademhosseini, A. Cell-laden microengineered gelatin methacrylate hydrogels. *Biomaterials* **2010**, *31* (21), 5536−5544.
(44) Zhang, G.; Huang, C.; Wang, R.; Guo, J.; Qin, Y.; Lv, S. Chondroprotective effects of Apolipoprotein D in knee osteoarthritis mice through the PI3K/AKT/mTOR signaling pathway. *Int. Immunopharmacol.* **2024**, *133*, 112005.
(45) Shi, X.; Jie, L.; Wu, P.; Zhang, N.; Mao, J.; Wang, P.; Yin, S. Calycosin mitigates chondrocyte inflammation and apoptosis by inhibiting the PI3K/AKT and NF-κB pathways. *J. Ethnopharmacol.* **2022**, *297*, 115536.
(46) Qin, M.; Jin, J.; Saiding, Q.; Xiang, Y.; Wang, Y.; Sousa, F.; Sarmento, B.; Cui, W.; Chen, X. In situ inflammatory-regulated drug-loaded hydrogels for promoting pelvic floor repair. *J. Controlled Release* **2020**, *322*, 375−389.

https://doi.org/10.1021/acsomega.4c07489
ACS Omega 2024, 9, 49597−49608